JOURNAL OF THEORETICAL AND APPLIED MECHANICS
57, 3, pp. 739-750, Warsaw 2019
DOI: 10.15632/jtam-pl/110220

FREE VIBRATION OF A HYPER-ELASTIC MICROBEAM USING A NEW "AUGMENTED BIDERMAN MODEL"

Ardeshir Karami Mohammadi, Saeed Danaee Barforooshi
Faculty of Mechanical Engineering, Shahrood University of Technology, Shahrood, Iran
e-mail: akaramim@shahroodut.ac.ir; akaramim@yahoo.com; saeeddanaee@gmail.com

A new augmented Biderman model inspired by the modified couple stress theory has been introduced to investigate the size effect in addition to nonlinear material effects. Then, this model is used to investigate free vibration of a hyper-elastic microbeam. Classical Biderman strain energy does not include the effect of small size in hyper-elastic materials. In order to consider the effect of small size, terms inspired by the modified couple stress theory are added to the classical Biderman strain energy function. In order to provide the possibility of calculating these terms, a relation between the material constants in the hyper-elastic Biderman model and the linear elastic constants is obtained. The equations of motion of the microbeam is obtained based on the extended Hamilton principle, and then is solved using Galerkin discretization and perturbation methods. The effect of thickness to length scale ratio on the normalized frequency is studied for different modes. It is shown that when thickness gets larger in comparison with the length scale parameter, the normalized frequency tends to classical Biderman results. The results obtained are validated by results of the Runge-Kutta numerical method and indicate an excellent agreement. Mode shapes of the microbeam based on the classical and the augmented models are depicted, where the augmented model anticipates stiffer behavior for hyperelastic microbeams.

Keywords: nonlinear vibration, hyper-elastic microbeam, augmented Biderman model, modified couple stress theory

1. Introduction

Dielectric Elastomers (DEs) made of hyper-elastic materials fitted between two compatible electrodes were discovered in the early 1990's (Perline *et al.*, 2002). These materials have recently attracted much attention. Some of their special features include high strain, low cost, simplicity of structure, robustness due to the use of stable and commercially available polymer materials, high energy production (Mockensturm and Goulbourne, 2006; Feng *et al.*, 2014; Carpi *et al.*, 2011). These have made it possible to make devices such as artificial muscles sensors, actuators, generators and energy harvesting devices (Löwe *et al.*, 2005; Chakravarty, 2014; Feng *et al.*, 2011; Zhang *et al.*, 2005).

An important advantage of a dielectric elastomer used in the resonator – in comparison to conventional silicon – is easy adjusting just after manufacturing (Zhang *et al.*, 2005; Ogden and Roxburgh, 1993). The dielectric elastomer includes material nonlinearity and it should be modeled properly. Few articles are reported in accounting this property, and majority of them deal only with geometric nonlinearity. Some of these articles are presented here.

Verron *et al.* (1999) analyzed dynamic inflation of hyper-elastic spherical membranes of a Mooney-Rivlin material. Also they examined oscillatory inflation around the static fixed point and found that, for a given material, the frequency of oscillation exhibited a maximum at some pressure level, which tended to increase for materials closer to neo-Hookean behavior.

Dubois *et al.* (2008) presented modeling of the first mode resonance frequency of a dielectric electro-active polymer membrane. They deduced that the electrostatic force from the applied voltage effectively softened the device and reduced its resonance frequency, in principle to zero at the buckling threshold. In addition, an excellent agreement was found between the measurements. An analytical model was developed based on the Rayleigh-Ritz theory.

Zhang *et al.* (2005) constructed a micro-bridge polymer resonator. They showed that the quality factor in the vacuum would be about 100, which would be reduced by increasing air pressure as a result of air damping.

Soares and Gonçalves (2012) presented mathematical modeling of the nonlinear vibration of a prestretched hyperelastic annular membrane under finite deformation. The membrane material was assumed homogeneous, isotropic and neo-Hookean. They obtained vibration modes and frequencies of the hyper-elastic membrane by analytical and numerical methods and then reduced the order of the models for noneonlinear dynamic analysis, which was achieved by the Galerkin method. They used the finite element model to check the accuracy of the reduced order model.

Danaee Barforooshi and Karami Mohammadi (2016) considered a hyperelastic microbeam with geometric and material nonlinearity. Geometric nonlinearity was introduced by von Kármán and Yeoh, and neo-Hookean models were used for the material nonlinearity. They showed that the neo-Hookean model was not suitable for this case because of insufficient terms in its strain-energy function. They used a perturbation technique for solving the nonlinear governing equation and achieved a good agreement between analytical and numerical results. They showed a significant effect of the number of modes on the normalized frequency where in higher modes the effect of the aspect ratio was also increased.

Karami Mohammadi and Danaee Barforooshi (2017) studied nonlinear forced vibration of microbeams made of a dielectric elastomer. Hyperelastic Yeoh model was used to consider nonlinear behavior of the material, and solving the governing equations was done using the multiple scales method. The results obtained from the frequency response indicated that the microbeam had hardening behavior and the hardening was more intense in higher modes. When the mode number increased, the amplitude decreased, and the amplitude of the force had a direct effect on the start of bifurcation.

Several non-classical theories have been introduced to incorporate size dependency in linear elasticity, such as couple stress theory (Mindlin and Tiersten, 1962), strain gradient (Akgöz and Civalek, 2013; Abbasi and Mohammadi, 2014), nonlocal elasticity (Eringen, 1972; Aranda-Ruiz *et al.*, 2012), and a modified couple stress theory (Yang *et al.*, 2002).

Ke *et al.* (2012) proposed a Mindlin microplate model for vibration analysis of elastic microplates. The governing equations and boundary conditions were derived using the Hamilton principle. They studied the influence of the length scale parameter, side-to-thickness ratio and the aspect ratio on free vibration of the microplate. They found that size effect was only important at small ratios of the length scale parameter to thickness.

Kahrobaiyan *et al.* (2014) derived governing equations of a Timoshenko elastic beam based on the modified couple stress theory. They evaluated static deflection of a short beam and pull-in voltage of an electrostatically actuated silicon microcantilever by the proposed method. Final results were compared with those of FEM and a good agreement was achieved between them.

Wang *et al.* (2015) described nonlinear bending and thermal post-buckling of an Euler-Bernoulli elastic beam in accordance with the modified couple stress theory. They formulated the governing equation of motion through the equilibrium of an infinitesimal element including the size effect and von Kármán nonlinear theory. It was shown that the microbeam behaved relatively stiffer by incorporating the size effect and Poisson's ratio.

So far, no researcher has proposed a model for hyperelastic beam that incorporates the effect of small size, and such a model has not yet been developed.

In this paper, a new augmented Biderman model inspired by the modified couple stress theory has been introduced to investigate the size effect in addition to the nonlinear material effects. Then, this model is used to investigate free vibration of a hyper-elastic microbeam. In order to consider the effect of small size, terms inspired by the modified couple stress theory are added to the classical Biderman strain energy function. In order to provide the possibility of calculating these terms, a relation between material constants in the hyper-elastic Biderman model and linear elastic constants is obtained. The equations of motion of the microbeam is obtained based on the extended Hamilton principle, and then is solved using Galerkin discretization and perturbation methods. The effect of the thickness to length scale ratio on the normalized frequency is studied for different modes. It is shown that when thickness gets larger in comparison with the length scale parameter, the normalized frequency tends to classical Biderman results. The results obtained are validated by the results from the Runge-Kutta numerical method and indicate an excellent agreement. Mode shapes of the microbeam based on the classical and the augmented models are depicted, where the augmented model anticipates stiffer behavior for hyperelastic microbeams.

2. Basics of the modified couple stress theory

According to the modified couple stress theory developed by Yang *et al.* (2002), the strain energy density is a function of both strain and curvature tensors. The strain energy of an elastic continuum occupying the volume V is given as

$$\Pi = \frac{1}{2}\int_V (\boldsymbol{\sigma} : \boldsymbol{\varepsilon} + \mathbf{m} : \boldsymbol{\chi})\, dV \tag{2.1}$$

where $\boldsymbol{\sigma}$, $\boldsymbol{\varepsilon}$, $\mathbf{m}$ and $\boldsymbol{\chi}$ refer to classical stress, strain tensors, deviatoric part of the couple stress tensor and the symmetric curvature tensor, respectively. These tensors are defined by (Yang *et al.*, 2002)

$$\begin{aligned} &\boldsymbol{\sigma} = \lambda \operatorname{tr}(\boldsymbol{\varepsilon})\mathbf{I} + 2\mu\boldsymbol{\varepsilon} \qquad \varepsilon_{ij} = \frac{1}{2}\Big(\frac{\partial u_i}{\partial x_j} + \frac{\partial u_j}{\partial x_i} + \frac{\partial u_k}{\partial x_j}\frac{\partial u_k}{\partial x_i}\Big) \\ &\mathbf{m} = 2\mu l^2 \boldsymbol{\chi} \qquad \boldsymbol{\chi} = \frac{1}{2}(\boldsymbol{\theta}\otimes\nabla + \nabla\otimes\boldsymbol{\theta}) \end{aligned} \tag{2.2}$$

where $\mathbf{u}$ is the displacement and $\boldsymbol{\theta}$ is the rotation vector defined as

$$\boldsymbol{\theta} = \frac{1}{2}\operatorname{curl}(\mathbf{u}) \tag{2.3}$$

It should be mentioned that l stands for the length scale parameter.

3. Augmented Biderman model

The Biderman model is one of the polynomial models that include terms for $i = 0$ or $j = 0$ in the Mooney-Rivlin model. This model has three terms for I_1 and a term for I_2 (Marckmann and Verron, 2006)

$$W = c_{10}(I_1 - 3) + c_{01}(I_2 - 3) + c_{20}(I_1 - 3)^2 + c_{30}(I_1 - 3)^3 \tag{3.1}$$

In order to consider the effect of small size on behavior of hyperelastic components such as microbeams, Equation (2.1) and the terms related to $\mathbf{m}$ and $\boldsymbol{\chi}$ are added to the Biderman

model, so a novel "augmented Biderman model" inspired by the modified couple stress theory is introduced as

$$\Pi = \int_V [c_{10}(I_1 - 3) + c_{01}(I_2 - 3) + c_{20}(I_1 - 3)^2 + c_{30}(I_1 - 3)^3 + m_{xy}\chi_{xy}]\, dV \tag{3.2}$$

In order to determine the components of $\mathbf{m}$, due to Equation $(2.2)_3$, the shear modulus μ is estimated according to the Biderman constants of Eq. (3.1).

The test considered here is the uniaxial tension, so the stress components should be introduced as

$$\boldsymbol{\sigma}_1 = \boldsymbol{\sigma} \qquad \boldsymbol{\sigma}_2 = \boldsymbol{\sigma}_3 = \mathbf{0} \tag{3.3}$$

The stress-strain relation for hyper-elastic materials is

$$\sigma_{ij} = -p\delta_{ij} + 2\Big(\frac{\partial W}{\partial I_1}\Big)_{I_1=3} C_{ij} - 2\frac{\partial W}{\partial I_2}\frac{1}{C_{ij}} \tag{3.4}$$

On the other hand, the right Cauchy-Green deformation tensor is

$$\mathbf{C} = \mathbf{F}^{\mathrm{T}}\mathbf{F} = \begin{bmatrix} 2\varepsilon_{11} + 1 & 0 & 2\varepsilon_{13} \\ 0 & 1 & 0 \\ 2\varepsilon_{13} & 0 & 1 \end{bmatrix} \tag{3.5}$$

and the stress constants could be written as

$$\begin{aligned} I_1 &= \operatorname{tr}(\mathbf{C}) = 2\varepsilon_{xx} + 3 \\ I_2 &= \frac{1}{2}[\operatorname{tr}(C)^2 - \operatorname{tr}(C^2)] = 4\varepsilon_{xx} - 4\varepsilon_{xz}^2 + 3 \end{aligned} \tag{3.6}$$

Applying (3.3) into (3.4) leads to

$$\sigma_{ij} = 2\Big(\frac{\partial W}{\partial I_1}\Big)_{I_1=3}(C_{ij} - \delta_{ij}) + 2\frac{\partial W}{\partial I_2}\Big(\delta_{ij} - \frac{1}{C_{ij}}\Big) \tag{3.7}$$

Writing Equation (3.7) in a suitable form and using equations (3.1), (3.5) and (3.6) leads to the shear stress and shear strain relation as

$$\tau_{13} = 4(c_{10} + c_{01})\varepsilon_{13} \tag{3.8}$$

where $4(c_{10} + c_{01})$ plays the role of the shear modulus μ.

4. Governing equations

In this Section, governing equations of motion are derived based on the new "augmented Biderman model" (3.2). It should be mentioned that a simply-supported hyper elastic microbeam has length L , height d and width b, as it is shown in Fig. 1.

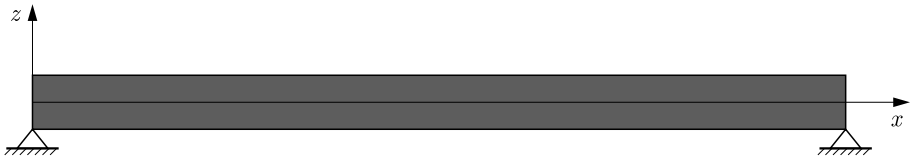

Fig. 1. Schematic of the microbeam

Displacement components are described as

$$u = -z\phi(x,t) \qquad v = 0 \qquad w = w(x,t) \tag{4.1}$$

Due to large deformation, Lagrange strain tensor should be used. Therefore, according to Eq. $(2.2)_2$, its components are

$$\varepsilon_{xx} = -z\frac{\partial\phi}{\partial x} + \frac{1}{2}\Big(\frac{\partial w}{\partial x}\Big)^2 \qquad \varepsilon_{xz} = \varepsilon_{zx} \simeq \frac{1}{2}\Big(\frac{\partial w}{\partial x} - \phi\Big) \tag{4.2}$$

All other strain components are zero.

The only non-zero components of the symmetric curvature tensor will be

$$\chi_{xy} = \chi_{yx} = -\frac{1}{4}\Big(\frac{\partial^2 w}{\partial x^2} + \frac{\partial\phi}{\partial x}\Big) \tag{4.3}$$

To investigate the governing equations of motion, kinetic energy is

$$T = \frac{\rho}{2}\int_0^l \Big[I\Big(\frac{\partial\phi}{\partial t}\Big)^2 + A\Big(\frac{\partial w}{\partial t}\Big)^2\Big]\,dx \tag{4.4}$$

And for potential energy, the novel "augmented Biderman model" (3.2) is applied

$$\Pi = \int_V [c_{10}(I_1-3) + c_{01}(I_2-3) + c_{20}(I_1-3)^2 + c_{30}(I_1-3)^3 + m_{xy}\chi_{xy}]\,dV \tag{4.5}$$

Applying Eqs. (4.4) and (4.5) into the extended Hamilton principle, the final governing equations are achieved

$$\begin{aligned}
&\rho I\frac{\partial^2\phi}{\partial t^2} - 2c_{01}A\phi + 2c_{01}A\frac{\partial w}{\partial x} - \Big(8c_{20}I + \frac{\mu l^2 A}{4}\Big)\frac{\partial^2\phi}{\partial x^2}\\
&\quad - 24c_{30}I\Big[\frac{\partial^2\phi}{\partial x^2}\Big(\frac{\partial w}{\partial x}\Big)^2 + 2\frac{\partial^2 w}{\partial x^2}\frac{\partial w}{\partial x}\frac{\partial\phi}{\partial x}\Big] - \frac{\mu l^2 A}{4}\frac{\partial^3 w}{\partial x^3} = 0\\
&\rho A\frac{\partial^2 w}{\partial t^2} - (2c_{10}+2c_{01})A\frac{\partial^2 w}{\partial x^2} - 2c_{01}A\frac{\partial\phi}{\partial x} - 12c_{20}A\frac{\partial^2 w}{\partial x^2}\Big(\frac{\partial w}{\partial x}\Big)^2 - 30c_{30}A\Big(\frac{\partial w}{\partial x}\Big)^4\frac{\partial^2 w}{\partial x^2}\\
&\quad - 24c_{30}I\Big[\frac{\partial^2 w}{\partial x^2}\Big(\frac{\partial\phi}{\partial x}\Big)^2 + 2\frac{\partial^2\phi}{\partial x^2}\frac{\partial\phi}{\partial x}\frac{\partial w}{\partial x}\Big] + \frac{\mu l^2 A}{4}\frac{\partial^4 w}{\partial x^4} + \frac{\mu l^2 A}{4}\frac{\partial^3\phi}{\partial x^3} = 0
\end{aligned} \tag{4.6}$$

Boundary conditions extracted from the Hamilton principle are

$$\begin{aligned}
&\text{at}\quad x = 0, L: \quad 2(c_{10}+c_{01})A\frac{\partial w}{\partial x} + 2c_{01}A\phi + 4c_{20}A\Big(\frac{\partial w}{\partial x}\Big)^3 + 6c_{30}A\Big(\frac{\partial w}{\partial x}\Big)^5\\
&\quad + 24c_{30}I\frac{\partial w}{\partial x}\Big(\frac{\partial\phi}{\partial x}\Big)^2 - \frac{\mu A l^2}{4}\Big(\frac{\partial^3 w}{\partial x^3} + \frac{\partial^2\phi}{\partial x^2}\Big) = 0 \qquad \text{or} \qquad \delta w = 0\\
&\text{at}\quad x = 0, L: \quad 8c_{20}I\frac{\partial\phi}{\partial x} + 24c_{30}I\frac{\partial\phi}{\partial x}\Big(\frac{\partial w}{\partial x}\Big)^2 + \frac{\mu A l^2}{4}\Big(\frac{\partial^2 w}{\partial x^2} + \frac{\partial\phi}{\partial x}\Big) = 0\\
&\quad \text{or} \qquad \delta\phi = 0
\end{aligned} \tag{4.7}$$

Boundary conditions chosen from Eqs. (4.7) for the simply supported beam are

$$\text{at}\quad x = 0, L: \quad w = 0 \quad \text{and} \quad 8c_{20}I\frac{\partial\phi}{\partial x} + 24c_{30}I\frac{\partial\phi}{\partial x}\Big(\frac{\partial w}{\partial x}\Big)^2 + \frac{\mu A l^2}{4}\Big(\frac{\partial^2 w}{\partial x^2} + \frac{\partial\phi}{\partial x}\Big) = 0 \tag{4.8}$$

Equations (4.6) can be written in a non-dimensioned form by introducing the following parameters

$$x^* = \frac{x}{L} \qquad w^* = \frac{w}{d} \qquad t^* = t\omega_{dim} \qquad \phi^* = \phi \tag{4.9}$$

where ω_{dim} is the natural frequency of the linear Euler-Bernoulli microbeam.

Substituting these parameters into Eqs. (4.6), non-dimensional governing equations can be introduced as (the stars are removed for simplicity)

$$\begin{aligned}
&\frac{\partial^2\phi}{\partial t^2}-\beta_1\phi+\beta_2\frac{\partial w}{\partial x}-\beta_3\frac{\partial^2\phi}{\partial x^2}-\beta_4\Big[\frac{\partial^2\phi}{\partial x^2}\Big(\frac{\partial w}{\partial x}\Big)^2+2\frac{\partial^2 w}{\partial x^2}\frac{\partial w}{\partial x}\frac{\partial\phi}{\partial x}\Big]-\beta_5\frac{\partial^3 w}{\partial x^3}=0\\
&\frac{\partial^2 w}{\partial t^2}-\beta_6\frac{\partial^2 w}{\partial x^2}-\beta_7\frac{\partial\phi}{\partial x}-\beta_8\frac{\partial^2 w}{\partial x^2}\Big(\frac{\partial w}{\partial x}\Big)^2-\beta_9\Big(\frac{\partial w}{\partial x}\Big)^4\frac{\partial^2 w}{\partial x^2}\\
&\quad-\beta_{10}\Big[\frac{\partial^2 w}{\partial x^2}\Big(\frac{\partial\phi}{\partial x}\Big)^2+2\frac{\partial^2\phi}{\partial x^2}\frac{\partial\phi}{\partial x}\frac{\partial w}{\partial x}\Big]+\beta_{11}\frac{\partial^4 w}{\partial x^4}+\beta_{12}\frac{\partial^3\phi}{\partial x^3}=0
\end{aligned}\tag{4.10}$$

where

$$\begin{aligned}
&\beta_1=\frac{2c_{01}A}{\rho I\omega_{dim}^2} \qquad \beta_2=\frac{2c_{01}Ad}{\rho IL\omega_{dim}^2} \qquad \beta_3=\frac{32c_{20}I+\mu Al^2}{4\rho L^2\omega_{dim}^2} \qquad \beta_4=\frac{24c_{30}d^2}{\rho L^4\omega_{dim}^2}\\
&\beta_5=\frac{\mu Al^2d}{4\rho L^3I\omega_{dim}^2} \qquad \beta_6=\frac{2c_{10}+2c_{01}}{\rho L^2\omega_{dim}^2} \qquad \beta_7=\frac{2c_{01}}{\rho Ld\omega_{dim}^2} \qquad \beta_8=\frac{12c_{20}d^2}{\rho L^4\omega_{dim}^2}\\
&\beta_9=\frac{30c_{30}d^4}{\rho L^6\omega_{dim}^2} \qquad \beta_{10}=\frac{24c_{30}I}{\rho Al^4\omega_{dim}^2} \qquad \beta_{11}=\frac{\mu l^2}{4\rho L^4\omega_{dim}^2} \qquad \beta_{12}=\frac{\mu l^2}{4\rho L^3d\omega_{dim}^2}
\end{aligned}$$

with the boundary conditions

$$\text{at}\quad x=0,1:\quad w=0\quad\text{and}\quad 8c_{20}I\frac{\partial\phi}{\partial x}+24c_{30}I\frac{\partial\phi}{\partial x}\Big(\frac{\partial w}{\partial x}\Big)^2+\frac{\mu Al^2}{4}\Big(\frac{\partial^2 w}{\partial x^2}+\frac{\partial\phi}{\partial x}\Big)=0 \tag{4.11}$$

5. Solution procedure

In order to investigate the nonlinear vibration of the microbeam, the Galerkin method with the first mode approximation can be employed. So the deflection of the microbeam can be assumed as $X(x)q(t)$, where $X(x)$ represents the first mode shape and $q(t)$ shows the time variable (Kahrobaiyan *et al.*, 2014)

$$\begin{aligned}
&\phi(x,t)=X_1(x)q_1(t) \qquad X_1(x)=\sqrt{2}\cos(m\pi x)\\
&w(x,t)=X_2(x)q_2(t) \qquad X_2(x)=\sqrt{2}\sin(m\pi x)
\end{aligned}\tag{5.1}$$

Using the Galerkin method and inserting Eqs. (5.1) into Eqs. (4.10) leads to two coupled equations with the time variable

$$\begin{aligned}
&\ddot{q}_1+(\beta_3m^2\pi^2-\beta_1)q_1+(\beta_2m\pi+\beta_5m^3\pi^3)q_2+\Big(\frac{\beta_4m^4\pi^4}{2}\Big)q_1q_2^2=0\\
&\ddot{q}_2-(\beta_6m^2\pi^2)q_2+(\beta_7m\pi)q_1+\Big(\frac{\beta_8m^4\pi^4}{2}\Big)q_2^3+\Big(\frac{\beta_9m^6\pi^6}{2}\Big)q_2^5\\
&\quad+\Big(\frac{\beta_{10}m^4\pi^4}{2}\Big)q_2q_1^2+(\beta_{11}m^4\pi^4)q_2^4+(\beta_{12}m^3\pi^3)q_1^3=0
\end{aligned}\tag{5.2}$$

Applying the transformed variable $\tau=\omega t$ to Eqs. (5.2) leads to

$$\begin{aligned}
&\omega^2\ddot{q}_1+\alpha_1q_1+\alpha_2q_2+\alpha_3q_1q_2^2=0\\
&\omega^2\ddot{q}_2+\alpha_4q_2+\alpha_5q_1+\alpha_6q_2^3+\alpha_7q_2^5+\alpha_8q_2q_1^2+\alpha_9q_2^4+\alpha_{10}q_1^3=0
\end{aligned}\tag{5.3}$$

which

$$\begin{aligned}
&\alpha_1=\beta_3m^2\pi^2-\beta_1 \qquad \alpha_2=\beta_2m\pi+\beta_5m^3\pi^3 \qquad \alpha_3=\frac{\beta_4m^4\pi^4}{2}\\
&\alpha_4=-\beta_6m^2\pi^2 \qquad \alpha_5=\beta_7m\pi \qquad \alpha_6=\frac{\beta_8m^4\pi^4}{2} \qquad \alpha_7=\frac{\beta_9m^6\pi^6}{2}\\
&\alpha_8=\frac{\beta_{10}m^4\pi^4}{2} \qquad \alpha_9=\beta_{11}m^4\pi^4 \qquad \alpha_{10}=\beta_{12}m^3\pi^3
\end{aligned}$$

In order to solve the equations using the perturbation method, the solutions can be expanded into series

$$\begin{aligned} q_1 &= \varepsilon q_{10} + \varepsilon^2 q_{11} + \varepsilon^3 q_{12} + \dots \\ q_2 &= \varepsilon q_{20} + \varepsilon^2 q_{21} + \varepsilon^3 q_{22} + \dots \\ \omega &= \omega_0 + \varepsilon\omega_1 + \varepsilon^2\omega_2 + \dots \end{aligned} \tag{5.4}$$

Substituting these solutions into equations (5.3), and separating the terms with different orders of ε, one can write

$$\omega_0^2\frac{\partial^2 q_{10}}{\partial\tau^2} + \alpha_1 q_{10} + \alpha_2 q_{20} = 0 \qquad \omega_0^2\frac{\partial^2 q_{20}}{\partial\tau^2} + \alpha_5 q_{10} + \alpha_4 q_{20} = 0 \tag{5.5}$$

and

$$\begin{aligned} &\omega_0^2\frac{\partial^2 q_{11}}{\partial\tau^2} + 2\omega_0\omega_1\frac{\partial^2 q_{10}}{\partial\tau^2} + \alpha_1 q_{11} + \alpha_2 q_{21} = 0 \\ &\omega_0^2\frac{\partial^2 q_{21}}{\partial\tau^2} + 2\omega_0\omega_1\frac{\partial^2 q_{20}}{\partial\tau^2} + \alpha_4 q_{21} + \alpha_5 q_{11} = 0 \\ &\omega_0^2\frac{\partial^2 q_{12}}{\partial\tau^2} + 2\omega_0\omega_1\frac{\partial^2 q_{11}}{\partial\tau^2} + (2\omega_0\omega_2 + \omega_1^2)\frac{\partial^2 q_{10}}{\partial\tau^2} + \alpha_1 q_{12} + \alpha_2 q_{22} + \alpha_3 q_{20}^2 q_{10} = 0 \\ &\omega_0^2\frac{\partial^2 q_{22}}{\partial\tau^2} + 2\omega_0\omega_1\frac{\partial^2 q_{21}}{\partial\tau^2} + (2\omega_0\omega_2 + \omega_1^2)\frac{\partial^2 q_{20}}{\partial\tau^2} + \alpha_4 q_{22} + \alpha_5 q_{12} + \alpha_6 q_{20}^3 \\ &\quad + \alpha_8 q_{10}^2 q_{20} + \alpha_{10} q_{10}^3 = 0 \end{aligned} \tag{5.6}$$

To solve these equations, each pair of equations can be written in the following matrix form, for example for equations (5.5)

$$\begin{bmatrix} \ddot{q}_{10} \\ \ddot{q}_{20} \end{bmatrix} + \frac{1}{\omega_0^2}\begin{bmatrix} \alpha_1 & \alpha_2 \\ \alpha_5 & \alpha_4 \end{bmatrix}\begin{bmatrix} q_{10} \\ q_{20} \end{bmatrix} = \begin{bmatrix} 0 \\ 0 \end{bmatrix} \qquad \text{or} \qquad \ddot{\mathbf{q}}_0 + \mathbf{A}\mathbf{q}_0 = \mathbf{0} \tag{5.7}$$

The modal coordinates are defined as $\widehat{\mathbf{q}}$, which is related to $\mathbf{q}_0$ coordinates using the modal matrix $\mathbf{V}$, as $\widehat{\mathbf{q}} = \mathbf{V}^{-1}\mathbf{q}_0$ or $\mathbf{q}_0 = \mathbf{V}\widehat{\mathbf{q}}$. So Eq. (5.7) can be written as follows

$$\mathbf{V}\ddot{\widehat{\mathbf{q}}} + \mathbf{A}\mathbf{V}\widehat{\mathbf{q}} = \mathbf{0} \tag{5.8}$$

By premultiplying $\mathbf{V}^{-1}$ in Eq. (5.8), and using well-known equation $\mathbf{V}^{-1}\mathbf{A}\mathbf{V} = \mathbf{\Lambda}$, the result is

$$\ddot{\widehat{\mathbf{q}}}_0 + \mathbf{\Lambda}\widehat{\mathbf{q}} = \mathbf{0} \tag{5.9}$$

where $\mathbf{\Lambda}$ is a diagonal matrix. With the initial conditions $\widehat{q}_1(0) = 0$, $\dot{\widehat{q}}_1(0) = 0$, $\widehat{q}_2(0) = \widetilde{w}_{max} = w/d$, $\dot{\widehat{q}}_2(0) = 0$ the answer to Eq. (5.5) is

$$q_{10} = v_{12}\widetilde{w}_{max}\cos(\omega_0\tau) \qquad q_{20} = v_{22}\widetilde{w}_{max}\cos(\omega_0\tau) \tag{5.10}$$

where v_{12} and v_{22} are elements of the second eigenvector.

Inserting Eqs. (5.10) into $(5.12)_2$ leads to secular terms, and eliminating these terms, gives

$$\omega_1 = 0 \qquad q_{21} = 0 \tag{5.11}$$

Inserting Eqs. (5.10) and (5.11) into $(5.6)_3$ and $(5.6)_4$ leads to

$$\begin{aligned} \omega_0^2\ddot{q}_{22} + \alpha_5 q_{12} + \alpha_4 q_{22} &= 2\omega_0^3\omega_2 V_{22}\widetilde{w}_{max}\cos(\omega_0\tau) - (\alpha_8 V_{22}V_{12}^2 + \alpha_6 V_{22}^3)\widetilde{w}_{max}^3\cos^3(\omega_0\tau) \\ \omega_0^2\ddot{q}_{12} + \alpha_1 q_{12} + \alpha_2 q_{22} &= 2\omega_0^3\omega_2 V_{12}\widetilde{w}_{max}\cos(\omega_0\tau) - (\alpha_3 V_{12}V_{22}^2)\widetilde{w}_{max}^3\cos^3(\omega_0\tau) \end{aligned} \tag{5.12}$$

To solve Eqs. (5.12), the following solutions are proposed

$$\begin{aligned} q_{12} &= A_{11}\cos(\omega_0\tau) + A_{12}\cos(3\omega_0\tau) \\ q_{22} &= A_{21}\cos(\omega_0\tau) + A_{22}\cos(3\omega_0\tau) \end{aligned} \tag{5.13}$$

Applying Eqs. (5.13) to (5.12) and writing them as a matrix, gives

$$\begin{aligned} &\begin{bmatrix} \alpha_5 & \alpha_4 - \omega_0^4 \\ \alpha_1 - \omega_0^4 & \alpha_2 \end{bmatrix} \begin{bmatrix} A_{11} \\ A_{21} \end{bmatrix} = \begin{bmatrix} 2\omega_0^3\omega_2 V_{22}\widetilde{w}_{max} - \dfrac{3}{4}(\alpha_8 V_{22}V_{12}^2 + \alpha_6 V_{22}^3)\widetilde{w}_{max}^3 \\ 2\omega_0^3\omega_2 V_{12}\widetilde{w}_{max} - \dfrac{3}{4}(\alpha_3 V_{12}V_{22}^2)\widetilde{w}_{max}^3 \end{bmatrix} \\ &\begin{bmatrix} \alpha_5 & \alpha_4 - \omega_0^4 \\ \alpha_2 & \alpha_1 - \omega_0^4 \end{bmatrix} \begin{bmatrix} A_{12} \\ A_{22} \end{bmatrix} = \begin{bmatrix} -\dfrac{1}{4}(\alpha_8 V_{22}V_{12}^2 + \alpha_6 V_{22}^3)\widetilde{w}_{max}^3 \\ -\dfrac{1}{4}(\alpha_3 V_{12}V_{22}^2)\widetilde{w}_{max}^3 \end{bmatrix} \end{aligned} \tag{5.14}$$

Substituting the elements of the right hand side of Eq. $(5.14)_1$ into the first column of the coefficient matrix and equating its determinant to zero enables finding ω_2

$$\omega_2 = \frac{3\alpha_2\widetilde{w}_{max}^2(\alpha_8 V_{12}^2 V_{22} + \alpha_6 V_{22}^3 + \alpha_{10}V_{12}^3) - 3\alpha_3\widetilde{w}_{max}^2(\alpha_4 - \omega_0^4)V_{22}^2 V_{12}}{8\alpha_2\omega_0^3 V_{22} - 8(\alpha_4 - \omega_0^4)\omega_0^3 V_{12}} \tag{5.15}$$

Also, substituting elements of the right hand side of Eq. $(5.14)_2$ instead of the first column of the coefficient matrix and again equation its determinant to zero yields ω_0

$$\omega_0^4 = \frac{\alpha_6 V_{22}^3(\alpha_4 - \alpha_2) + \alpha_4\alpha_3 V_{12}V_{22}^2 - \alpha_2\alpha_8 V_{12}^2 V_{22} - \alpha_2\alpha_{10}V_{12}^3}{9(\alpha_3 V_{12}V_{22}^2 + \alpha_6 V_{22}^3)} \tag{5.16}$$

6. Results

In this Section, shape modes of the microbeam in the classic and augmented Biderman models are introduced. Furthermore, the influence of d/l (thickness to the length scale parameter) on the normalized frequency ω/ω_c (augmented Biderman nonlinear frequency to the classical Biderman frequency) is investigated. This survey will be done for the microbeam with different single modes. The properties of the materials introduced in (Martins *et al.*, 2006), which are listed in Table 1, have been used for simulation.

Table 1. Properties of the microbeam

Geometric properties	Material properties (Martins *et al.*, 2006)
$L = 30\,\mu$m $b = 10\,\mu$m	$c_{01} = 2.33 \cdot 10^4$ Pa
	$c_{10} = 0.208$ MPa
	$c_{20} = -2.4 \cdot 10^3$ Pa
	$c_{30} = 5 \cdot 10^2$ Pa

In Figs. 2 to 4, the first, second and third shape modes of the classical and augmented Biderman models are shown. As evidenced in these figures, the augmented model predicts greater stiffness than the classical model.

Figures 5 to 7 show that in all modes, with an increase of the ratio d/l in the augmented Biderman model, the calculated frequency approaches the results of the classic Biderman. It is also observed that the results of Runge-Kutta's numerical method are consistent with the results of the analytical method with high accuracy.

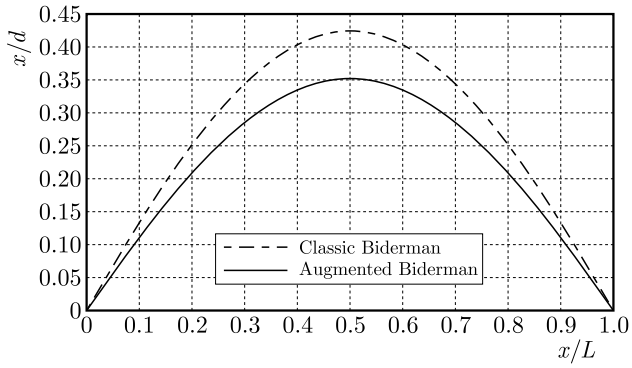

Fig. 2. The first shape mode in the classic and augmented Biderman models

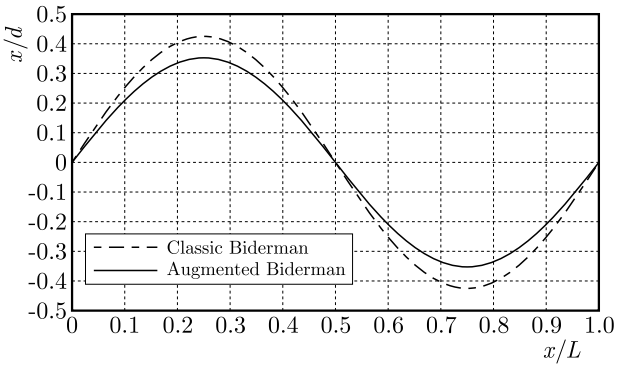

Fig. 3. The second shape mode in the classic and augmented Biderman models

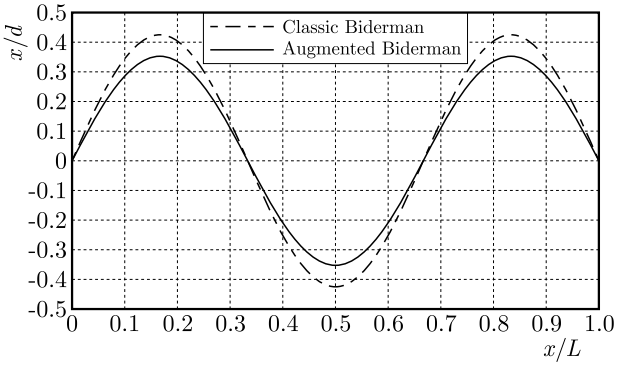

Fig. 4. The third shape mode in the classic and augmented Biderman models

7. Conclusions

In this research, a simply-supported hyperelastic microbeam has been considered. The von Kármán strain-displacement theory was applied for large deformation nonlinearity and a new augmented Biderman model inducted from the modified couple stress theory was introduced to consider material nonlinearity and the small scale effect. The Galerkin method and the Lindstedt-Poincaré procedure were used to solve the governing equation. Shape modes of the classic and augmented Bidermn models were described and it was shown that the microbeam had stiffer behavior in the augmented model. The influence of d/l on the normalized frequency was depicted for different modes. It was shown that in all modes, with an increase of the ratio d/l in the augmented Biderman model, the calculated frequency approached the results of the clas-

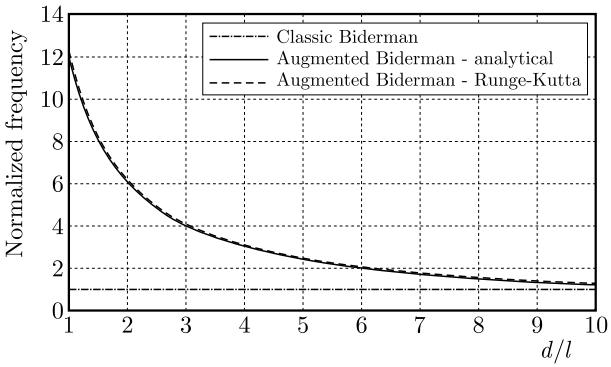

Fig. 5. Comparison between the augmented and classic Biderman models in terms of the normalized frequencies for the first mode

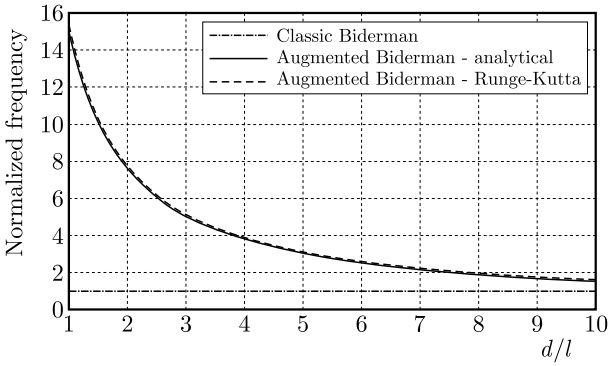

Fig. 6. Comparison between the augmented and classic Biderman models in terms of the frequencies for the second mode

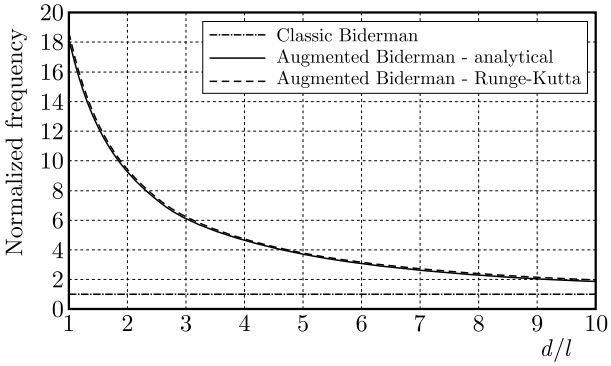

Fig. 7. Comparison between the augmented and classic Biderman models in terms of the normalized frequencies for the third mode

sic Biderman model. Validation of the results of the analytical method was carried out using Runge-Kutta's numerical method with high accuracy.

The strain energy of the classical Biderman model did not include the effect of small size in hyperelastic materials. A new augmented Biderman model inspired by the modified couple stress theory was introduced to investigate the size effect in addition to the nonlinear material effects. This augmented model, along with its results, can be a motivation for researchers to find values of the length scale parameters for the micro-parts made of hyperelastic materials using experimental methods.

References

1. Abbasi M., Mohammadi A.K., 2014, Study of the sensitivity and resonant frequency of the flexural modes of an atomic force microscopy microcantilever modeled by strain gradient elasticity theory, *Proceedings of the Institution of Mechanical Engineers, Part C: Journal of Mechanical Engineering Science*, **228**, 1299-1310
2. Akgöz B., Civalek Ö., 2013, A size-dependent shear deformation beam model based on the strain gradient elasticity theory, *International Journal of Engineering Science*, **70**, 1-14
3. Aranda-Ruiz J., Loya J., Fernández-Sáez J., 2012, Bending vibrations of rotating nonuniform nanocantilevers using the Eringen nonlocal elasticity theory, *Composite Structures*, **94**, 2990-3001
4. Carpi F., De Rossi D., Kornbluh R., Pelrine R.E., Sommer-Larsen P., 2011, *Dielectric Elastomers as Electromechanical Transducers: Fundamentals, Materials, Devices, Models and Applications of an Emerging Electroactive Polymer Technology*, Elsevier
5. Chakravarty U.K., 2014, On the resonance frequencies of a membrane of a dielectric elastomer, *Mechanics Research Communications*, **55**, 72-76
6. Danaee Barforooshi S., Karami Mohammadi A., 2016, Study neo-Hookean and Yeoh hyper--elastic models in dielectric elastomer-based micro-beam resonators, *Latin American Journal of Solids and Structures*, **13**, 1823-1837
7. Dubois P., Rosset S., Niklaus M., Dadras M., Shea H., 2008, Voltage control of the resonance frequency of dielectric electroactive polymer (DEAP) membranes, *Journal of Microelectromechanical Systems*, **17**, 1072-1081
8. Eringen A.C., 1972, Nonlocal polar elastic continua, *International Journal of Engineering Science*, **10**, 1-16
9. Feng C., Jiang L., Lau W.M., 2011, Dynamic characteristics of a dielectric elastomer-based microbeam resonator with small vibration amplitude, *Journal of Micromechanics and Microengineering*, **21**, 16-23
10. Feng C., Yu L., Zhang W., 2014, Dynamic analysis of a dielectric elastomer-based microbeam resonator with large vibration amplitude, *International Journal of Nonlinear Mechanics*, **65**, 63-68
11. Kahrobaiyan M.H., Asghari M., Ahmadian M.T., 2014, A Timoshenko beam model based on the modified couple stress theory, *International Journal of Mechanical Sciences*, **79**, 75-83
12. Karami Mohammadi A., Danaee Barforooshi S., 2017, Nonlinear forced vibration analysis of dielectric elastomer based microbeam with considering Yeoh hyper-elastic model, *Latin American Journal of Solids and Structures*, **14**, 643-656
13. Ke L.L., Wang Y.S., Yang J., Kitipornchai S., 2012, Free vibration of size-dependent Mindlin microplates based on the modified couple stress theory, *Journal of Sound and Vibration*, **331**, 94-106
14. Löwe C., Zhang X., Kovacs G., 2005, Dielectric elastomers in actuator technology, *Advanced Engineering Materials*, **7**, 361-367
15. Marckmann G., Verron E., 2006, Comparison of hyperelastic models for rubber-like materials, *Rubber Chemistry and Technology*, **79**, 835-858
16. Martins P.A.L., Natal Jorge R.M.A., Ferreira J.M.A., 2006, A comparative study of several material models for prediction of hyperelastic properties: application to silicone-rubber and soft tissues, *Strain*, **42**, 135-147
17. Mindlin R.D., Tiersten H.F., 1962, Effects of couple-stresses in linear elasticity, *Archive for Rational Mechanics and Analysis*, **11**, 415-448
18. Mockensturm E.M., Goulbourne N., 2006, Dynamic response of dielectric elastomers, *International Journal of Non-Linear Mechanics*, **41**, 388-395

19. Ogden R.W., Roxburgh D.G., 1993, The effect of pre-stress on the vibration and stability of elastic plates, *International Journal of Engineering Science*, **31**, 1611-1639

20. Perline R.E., Kornbluh R.D., Stanford P.Q., Oh S., Eckerle J., Full R.J., Rosenthal M.A., Meijer K., 2002, Dielectric elastomer artificial muscle actuator: toward biomimetic motion, *Proceeding of SPIE Electroactive Polymer Actuators and Devices*, 126-137

21. Soares R.M., Gonçalves P.B., 2012, Nonlinear vibrations and instabilities of a stretched hyperelastic annular membrane, *International Journal of Solids Structures*, **49**, 514-526

22. Verron E., Khayat R.E., Derdouri A., Peseux B., 1999, Dynamic inflation of hyperelastic spherical membrane, *Journal of Rheology*, **43**, 1083-1097

23. Wang Y.G., Lin W.H., Liu N., 2015, Nonlinear bending and post-buckling of extensible microscale beams based on modified couple stress theory, *Applied Mathematical Modeling*, **39**, 117-127

24. Yang F., Chong A., Lam D., Tong P., 2002, Couple stress based strain gradient theory for elasticity, *International Journal of Solids and Structures*, **39**, 2731-2743

25. Zhang G., Gaspar J., Chu V., Conde J.P., Electrostatically actuated polymer microresonators, *Applied Physics Letters*, **87**, 1-3

Manuscript received April 8, 2018; accepted for print April 3, 2019